



Measurement of the photon structure function at $\langle Q^2 \rangle = 700 \text{ GeV}^2$

I. Tyapkin N. Zimine, A. Zinchenko

Abstract

The photon structure function F_2^γ has been studied at average Q^2 values of 700 GeV^2 . The data correspond to the integrated luminosity of 548 pb^{-1} , collected by the DELPHI detector during the 1998-2000 LEP runs. Experimental distributions are compared with predictions of different Monte Carlo generators. The F_2^γ estimated from the fit of generated data to the experimental data and compared with theoretical expectations based on different models. A result for Q^2 evolution of the photon structure function has been obtained.

1 Introduction

In this paper measurements of the photon hadronic structure function are studied at high Q^2 in the reaction $e^+e^- \rightarrow e^+e^-X$, where X is a multihadronic system and when one of the scattered leptons is observed at a large scattering angle (tagging condition) while the other, remaining at a small angle, is undetected (anti-tagging condition). The data are compared to several different Monte Carlo generators to test these generators at high Q^2 . This reaction can be described as a deep inelastic $e\gamma$ scattering (DIS), where γ is almost a real photon. The corresponding cross-section can be expressed in terms of the photon structure functions $F_2^\gamma(x, Q^2)$ and $F_L(x, Q^2)$:

$$\frac{d\sigma}{dE_{tag}d\cos(\theta_{tag})} = \frac{4\pi\alpha^2 E_{tag}}{Q^4 y} \left[(1 + (1 - y)^2) F_2^\gamma(x, Q^2) - y^2 F_L(x, Q^2) \right]. \quad (1)$$

Here, E_{tag} and θ_{tag} are the energy and polar angle of the tagged lepton, $y=1 - (E_{tag}/E_{beam}) \cos^2 \theta_{tag}$, $Q^2=4E_{tag}E_{beam} \sin^2(\theta_{tag}/2)$, W is the invariant mass of the hadronic system, $x=Q^2/(Q^2 + W^2 + P^2)$ and P^2 is the negative four-momentum squared for the virtual photon emitted from the anti-tagged electron. Anti-tagging conditions ensures that P^2 is much smaller than Q^2 . But experimentally the influence of the real photon virtuality (P^2) is not negligible and photon structure function should be treated as a function of this value i.e. $F_2^\gamma(x, Q^2, P^2)$. Due to small values of y in the experimentally accessible region, an influence of F_L on the cross-section is small (about few percent) and may be taken into account in the simplified way given an additional uncertainty of these measurements.

The QCD description of F_2^γ divides into a perturbatively calculable part (point-like, anomalous) [1] and a non-perturbative 'hadronic part'. Several authors [1, 2, 3, 4, 5] have attempted to calculate F_2^γ . Difference in their approach have led to different predictions. At very high Q^2 non-perturbative part becoming small and different perturbative predictions can be compared.

2 Event generators

Three generators were used to produce simulated samples. A two-photon event generator TWOGAM [6] was successfully tested in previous DELPHI studies. The total cross-section is described by the sum of three parts: the point-like (QPM) component, resolved photon contribution (RPC) and soft hadronic (VDM) component. The QPM part based on the exact decomposition of the matrix element of the process and the exact differential cross-sections from [7] are used. The quark masses are taken to be 0.3 GeV for u and d quarks, 0.5 GeV for s and 1.6 GeV for c quarks. For the RPC perturbative part the lowest order cross-sections are used. Only the transverse-transverse part of the luminosity function is used in this case. There is no initial or final state parton showering. Strings are formed following the colour flow of the sub-processes. The remnant of a quark is an antiquark (and vice versa), and the remnant of a gluon is a $q\bar{q}$ pair. The produced system is fragmented as a string by JETSET 7.4 [8].

The Gordon-Storrow [2] parameterization were used in this analysis. A transverse momentum cutoff, $p_t^{cut}=1.8$ GeV, is applied to the partons of the resolved photons to separate soft from hard processes. In this analysis the GVDM structure function multiplied by the

factor $(1-x_{true})$ for the soft hadronic part was used. TWOGAM treats exactly the kinematics of the scattered electron and positron, and uses exact (unfactorised) expressions for the two photon luminosity function. New version of TWOGAM (2.04) was used in this analysis.

Second Monte Carlo event generator PHOJET [9] (version 1.12). hadronic multiparticle production at high energies. The generator includes the exact photon flux simulation for photon-photon processes in lepton-lepton collisions. The ideas and methods used in the program are based mainly on the Dual Parton Model (DPM). In order to combine the DPM on soft processes with the predictive power of perturbative QCD, the event generator is formulated as a two-component model (soft and hard components). On the basis of the optical theorem, Regge phenomenology is used to parametrise the total and elastic cross-sections as well as a series of partial inelastic cross-sections. In order to conserve s-channel unitarity, Gribov's Reggeon calculus is applied. Consequently, the model predicts so-called "multiple parton interactions" in one event. Since the unitarization of soft and hard processes is treated in unified way, multiple soft and hard interactions may be generated in one event. Hard scattering processes are simulated using lowest-order perturbative QCD. Initial state and final state parton showers are generated in leading-log approximation. Some coherence effects (angular ordering in the emissions) are taken into account. For the fragmentation of the parton configurations, the JETSET program is used.

Third Monte Carlo program used in this analysis is a PYTHIA (version 6.143) general purpose event generator. In this model different kinds of events distinguished as: direct events, VDM events and anomalous events [10]. In order that the above classification is smooth and free of double counting the cutoff parameters was introduced on the level of real photon fluctuation $\gamma \rightarrow q\bar{q}$ and the final hadronic system creation $\gamma\gamma^* \rightarrow q\bar{q}$. The VDM and anomalous events are together called resolved ones. But, this two classes differ in the structure of underlying event and in the appearance of soft events. The superposition of events mentioned above applies separately for each of the two incoming photons and forms six distinct classes of events: direct-direct, VDM-VDM, anomalous-anomalous, direct-VDM, direct-anomalous and VDM-anomalous. In the case of DIS only one of the photons can be resolved and only direct-direct, direct-VDM and direct-anomalous components should be taken in to account. This three contributions similar to the TWOGAM and PHOJET classification.

3 Event selection

The detailed description of the DELPHI detector can be found in [11]. The components of the detector relevant to the analysis of $\gamma\gamma$ events have been described in our previous papers [12], [13]. Data used in this analysis were collected with the DELPHI detector at the LEP e^+e^- collider during the 1998-2000 runs. The range of centre-of-mass energies is from 188 GeV to 208 GeV. The tagged particles were detected by the DELPHI electromagnetic calorimeter FEMC covering angular region from 10° to 40° .

The following criteria were used to select a sample of $\gamma\gamma^*$ events:

1. The energy deposited by the tagged electron (or positron) in the detector must be greater than $0.4 * E_{beam}$ (tagging requirement);

2. No additional clusters with energy exceeding $0.3 * E_{beam}$ must be observed anywhere in the forward calorimeters (anti-tagging requirement);
3. The track multiplicity is 4 or more. This includes only tracks with momenta greater than $0.25 \text{ GeV}/c$ with a polar angle between 20° and 160° and an impact parameter of less than 4 cm in the radial direction and less than 8 cm along the beam (hadronic final state selection);
4. The visible invariant mass of the hadronic system must be greater than 3 GeV and lower than 40 GeV;
5. The vector sum of transverse momenta of all particles, including tagged particle, normalised to E_{beam} must be less than 0.2;

Finally, a total of 524 events were selected. Which corresponds to visible cross-section of 0.97 pb. The background from $Z^0\gamma$ hadronic decays was estimated as 0.15 pb. The background from $\gamma\gamma^* \rightarrow \tau\tau$ interactions was estimated from a simulation as 0.05 pb. After subtraction of the background the visible cross-section of the investigated process was estimated as being 0.77 pb. The average Q^2 for the selected events is about 700 GeV^2 . The trigger efficiency was studied and found to be of the order of $99 \pm 0.5\%$.

4 Comparison of experimental and simulated data

To extract a measurement of the structure function from the data requires a reliable modelling of the process. There are few Monte Carlo generators in the market and only comparison between data and such generators may give some idea about reliability of the underlying physics.

All three generators mentioned above were used for the comparison with experimental distributions. The Q^2 , E_{tag}/E_{beam} and W_{vis} spectra are shown in Fig.1. One can see that TWOGAM and PYTHIA gives a reasonable description of the experimental data and PHOJET significantly overestimate visible cross-section. The observed x distribution is shown in Fig2. The experimental x distribution well reproduced by the TWOGAM and PYTHIA. Such an agreement means a good modelling of point-like component (dominating in this Q^2 region) by those generators. An over test of the final hadronic state modelling by the generators is the check of event topology. The energy flow versus pseudo-rapidity, defined as $\eta = -\ln(\tan(\theta/2))$, where θ is the polar angle of final state particles, is shown in Fig3.

It was observed since a very beginning that PHOJET have slightly wrong Q^2 dependence. This is not very important in the low Q^2 region and can be corrected but to be extrapolated in the Q^2 region under study led to the serious excess in PHOJET predictions. Later in this paper only TWOGAM and PYTHIA will be used.

5 Extraction of the structure function

In this analysis the MINUIT program is used. The correction factor A_{ij} is applied to each of the x_{true}^i (here i is a bin number, running from 1 to 2) for the simulated events and $x_{visible}$ Monte Carlo distribution fitted to the same data distribution. The correction factors A_{ij}

are the parameters for the fit. Such fit is performed for all possible combinations of ij , where j is running from 1 to 3 and reflecting the model (QPM, VDM, RPC). As a result, we have a set of structure functions extracted from the data with corresponding them reweighted distributions. The statistical analysis of these distributions gives χ^2 for each fit. This χ^2 is considered as a weight factor for $F_{2,ij}^\gamma$ measurement in each fit.

The difference in each x bin for different fits represents the systematic error due to the choice of the model or combinations of the models for the fit. Even the statistical error for each x bin depends on the choice of the model due to the different efficiency of event selection for each model. A combination of all fits gives the final result.

Results of the F_2^γ extraction with the use of two models are presented in Fig.4 and in the Table 1. The value of F_L^γ was estimated by TWOGAM and then taken into account in the final result. The same generator have been used to correct structure function extracted from the data for the non-zero virtuality of the target photon.

Model	x range	F_2^γ/α	Stat. err.	Mod. err.	Det. err.	Back. err.	Tot. Sys. err.	Tot. err.
1	0.01-0.3	1.011	0.084	0.104	0.148	0.122	0.217	0.231
2		0.582	0.095	0.154	0.139	0.111	0.235	0.253
1	0.3-0.8	0.940	0.050	0.077	0.072	0.024	0.108	0.119
2		0.984	0.055	0.089	0.068	0.020	0.114	0.126

Table 1. Summary for the F_2^γ estimated by the TWOGAM(1) and PYTHIA(2) generated data for the sample with average $Q^2=700 \text{ GeV}^2$.

The first error is the statistical one which in this approach also depends on the model, and in some sense, carries some systematic uncertainty. The model dependent shift in F_2^γ measured in each x bin was interpreted as a modelling systematics and is shown in the Table 1 in the fifth column. The shift of unfolding results due to variation in the selection criteria ($W_{min}, N_{min}^{trk} \dots$), thresholds for detection of neutrals by the calorimeters and uncertainty in the measurement of invariant mass was interpreted as a detector dependent systematic error. The background systematic error reflects an uncertainty in the knowledge of the background and was estimated from $Z^0\gamma$ hadronic and $\gamma\gamma \rightarrow \tau\tau$ Monte Carlo as an uncertainty with which we are able to describe the corresponding data samples. Certainly, there are some other sources of systematics in the measurements, but their influence is estimated as much lower. The correlation matrix for each of the presented results was checked. The maximum correlation between bins is found to be below 0.20.

Conclusions drawn from the result in the Table 1 are the following: 1. Taking into account total error both generators gives consistent results. 2. Results favour the GRV model prediction.

To study the Q^2 evolution of F_2^γ , results from the Table 1 taken with the use of TWOGAM. The only x intervals 0.3-0.8 used from this study.

The result is shown in Fig.5 together with the measurements made by other LEP collaborations [15, 21]. The function $a+b\text{Log}(Q^2)$ is fitted to the data taking into account the total errors. The results from LEP1 and LEP2 study with the STIC detector are taken into account. The results of the fit are shown in Table 2.

x range	a	da	b	db	χ^2/ndf
0.3-0.8	-0.032	0.071	0.343	0.046	0.37

Table 2. The Q^2 fit results.

Dependence consistent with linear function.

6 Conclusions

The photon hadronic structure function F_2^γ has been studied for the data taken by the DELPHI detector at LEP2 at $\sqrt{s_{ee}}=188-208$ GeV. The measurements are done in Q^2 interval from 200 to 2600 GeV² and in the x range from 0.01 to 0.8.

TWOGAM and PYTHIA Monte Carlo generators give reasonable description of the process and PHOJET fail to describe data.

Hadronic structure function estimated as a function of x in Q^2 interval, with mean momentum transfer $\langle Q^2 \rangle = 700$ GeV². The measurements of F_2^γ are found to be compatible with one constructed from the GRV- Set 2 parameterisation of the parton distributions of the photon. Combining the DELPHI data taken at $\sqrt{s_{ee}}=91$ GeV and 189-208 GeV, with different the $\langle Q^2 \rangle$ evolution of F_2^γ with Q^2 in the range $0.3 < x < 0.8$ has been measured. From this results the slope $\alpha^{-1}dF_2^\gamma/d\text{Log}(Q^2)$ is found to be consistent with the logarithmic evolution of F_2^γ with Q^2 .

7 Acknowledgements

We are greatly indebted to our technical collaborators and to the funding agencies for their support in building and operating the DELPHI detector, and to the members of the CERN SL Division for the excellent performance of the LEP collider.

References

- [1] M. Drees and R.M.Godbole, J. Phys. **G21** (1995) 1559.
- [2] L.E. Gordon and J.K. Storrow, Z.Phys. **C52** (1992) 307.
- [3] M. Gluck, E. Reya and A. Vogt, Phys. Rev. **D45** (1992) 3986.
- [4] H. Abramovicz, K. Charchula and A. Levy, Phys. Lett. **B269** (1991) 458.
- [5] G.A. Schuler and T. Sjostrand, Z. Phys. **C68** (1995) 607.
- [6] S. Nova, A. Olshevsky, T. Todorov, DELPHI-90-35 (unpublished).
- [7] V.N. Baier et al., Phys. Rep. **78** (1981) 293.
- [8] T. Sjöstrand, Comp. Phys. Comm. **82** (1994) 74.
- [9] Humboldt University, D-10099 Berlin, FRG.
- [10] Workshop on Physics at LEP2 ,CERN 96-01 v2 (1996).
- [11] DELPHI Coll. , P. Aarnio et al., Nucl. Instr. and Meth., **A303** (1991), 233.
- [12] DELPHI Coll., P. Abreu et al. Z.Phys. **C69** (1996) 223.

- [13] DELPHI Coll., P.Abreu et al., Phys.Lett. **B342** (1995) 402.
- [14] OPAL Collab., R. Akers et al., Z.Phys. **C61** (1994) 199.
- [15] OPAL Coll., K. Ackerstaff et al., Z.Phys. **C74** (1997) 33.
- [16] OPAL Coll., K. Ackerstaff et al., Phys. Lett. **B411** (1997) 387.
- [17] OPAL Coll., K. Ackerstaff et al., Phys. Lett. **B412** (1997) 225.
- [18] OPAL Coll., G. Abbiendi et al., Eur. Phys. J. **C18** (2000) 15.
- [19] L3 Coll., M. Acciarri et al., Phys. Lett. **B436** (1998) 403.
- [20] L3 Coll., M. Acciarri et al., Phys. Lett. **B447** (1999) 147.
- [21] L3 Coll., M. Acciarri et al., Phys. Let. **B483** (2000) 373.

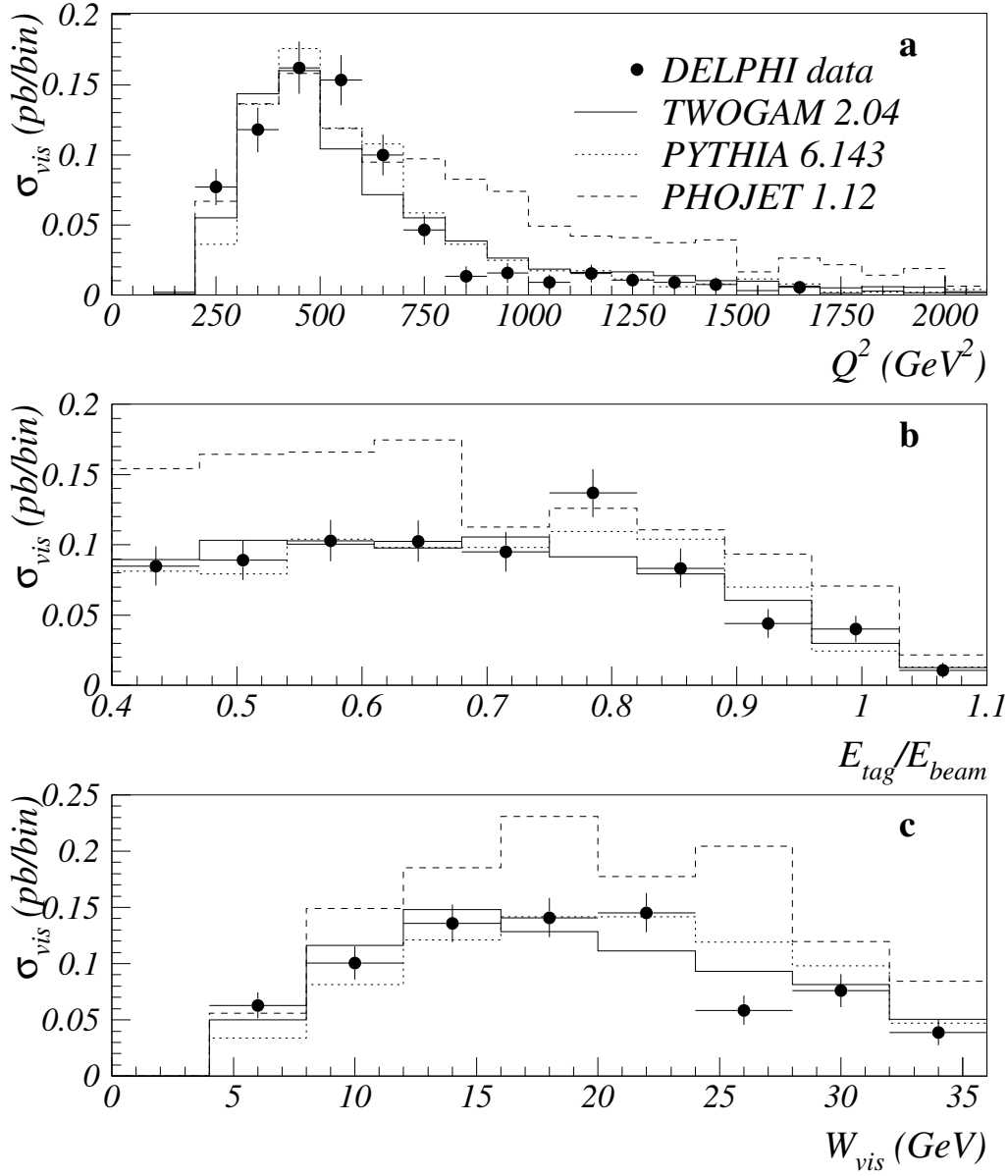


Figure 1: Comparison between data and Monte Carlo predictions for the sample with $\langle Q^2 \rangle = 40 \text{ GeV}^2$: a) Q^2 , b) tagging energy, c) invariant mass. Points are data and the lines show the Monte Carlo predictions from TWOGAM (solid line), PHOJET (dashed line) and PYTHIA (dotted line).

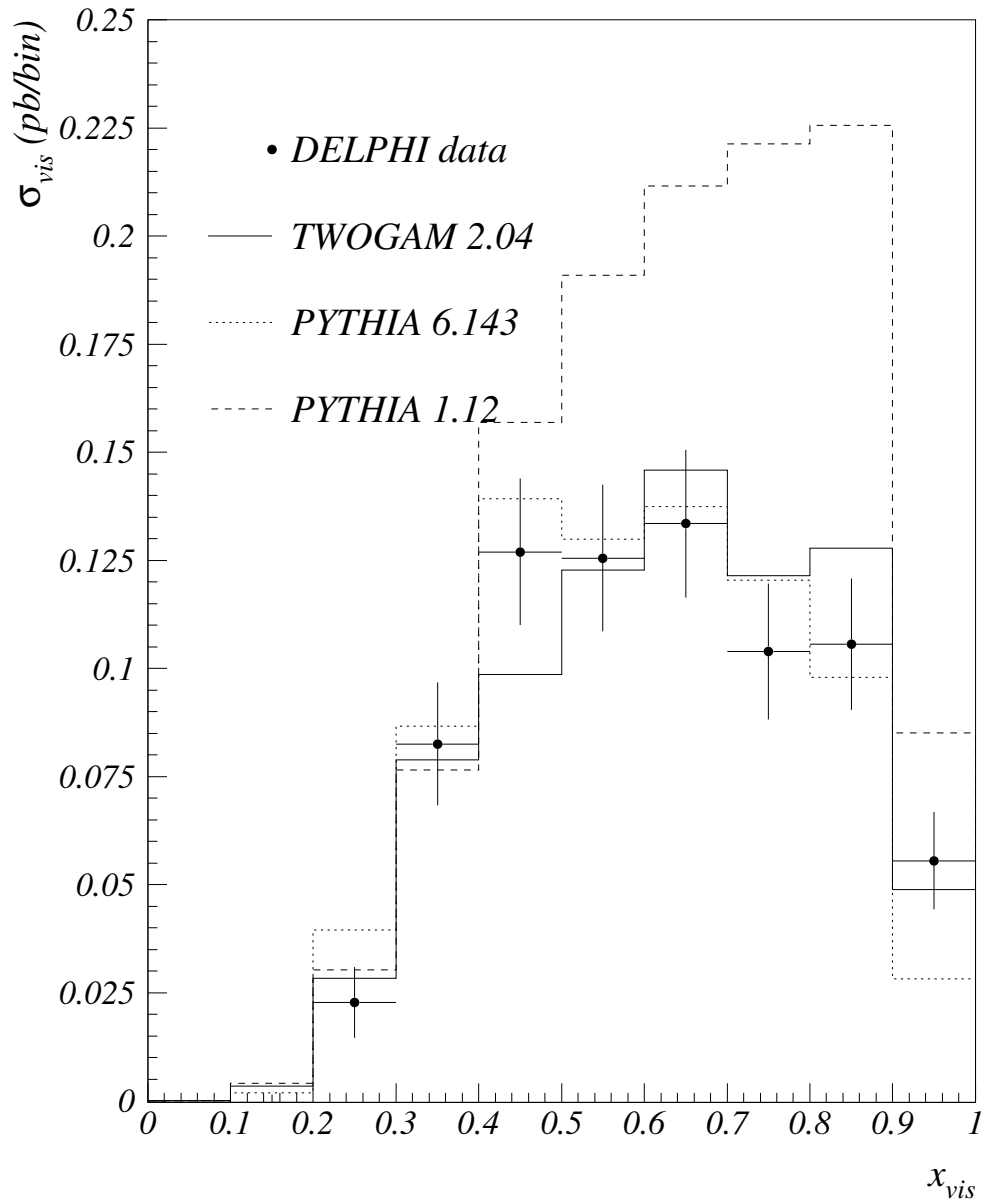


Figure 2: Comparison between data and Monte Carlo predictions for the x visible distributions. Points are data and the lines show the Monte Carlo predictions from TWOGAM (solid line), PHOJET (dashed line) and PYTHIA (dotted line).

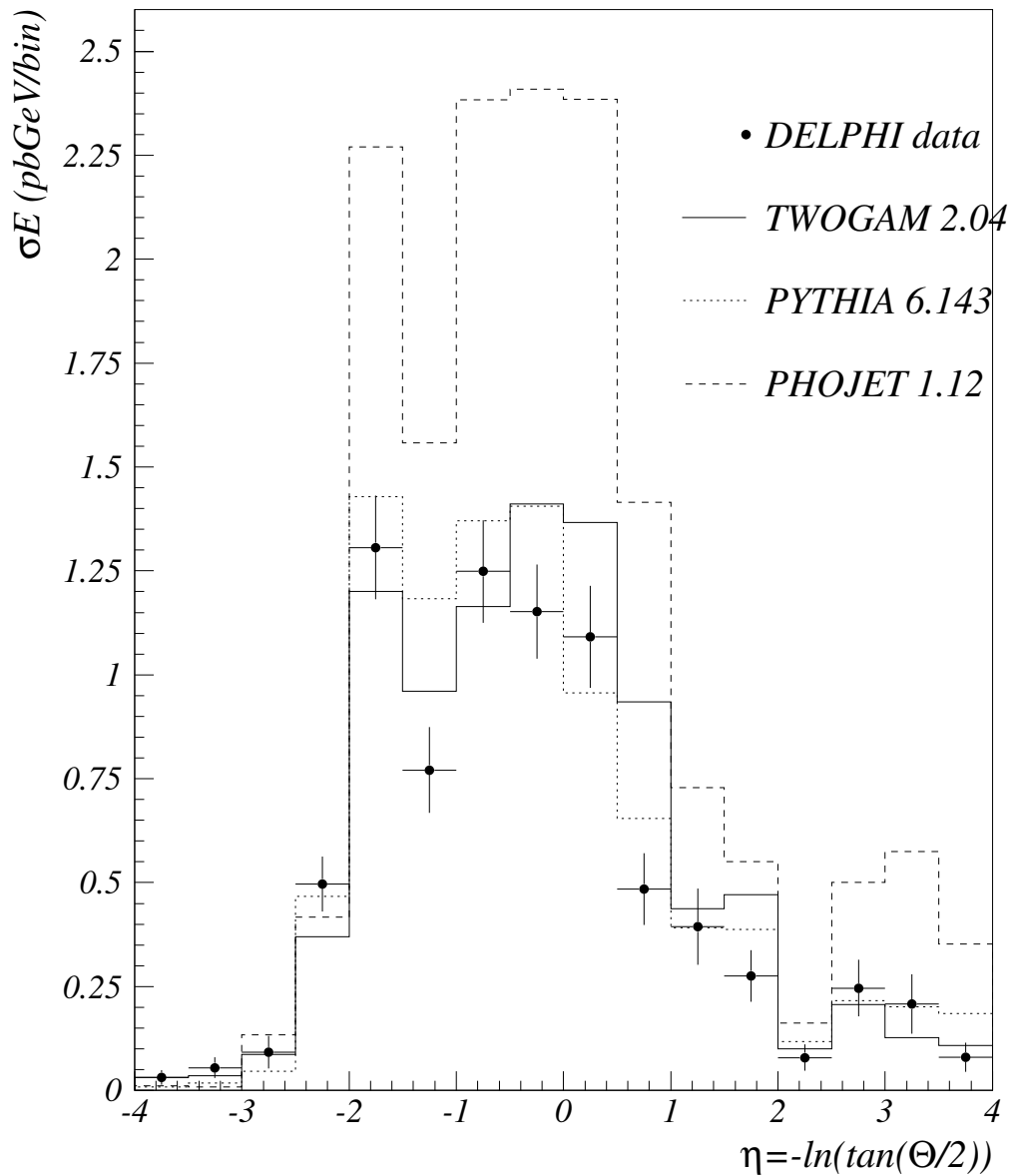


Figure 3: Comparison of hadronic energy flow for data and Monte Carlo prediction in the pseudorapidity scale for the selected events. Points are data and the lines show the Monte Carlo predictions from TWOGAM (solid line), PHOJET (dashed line) and PYTHIA (dotted line).

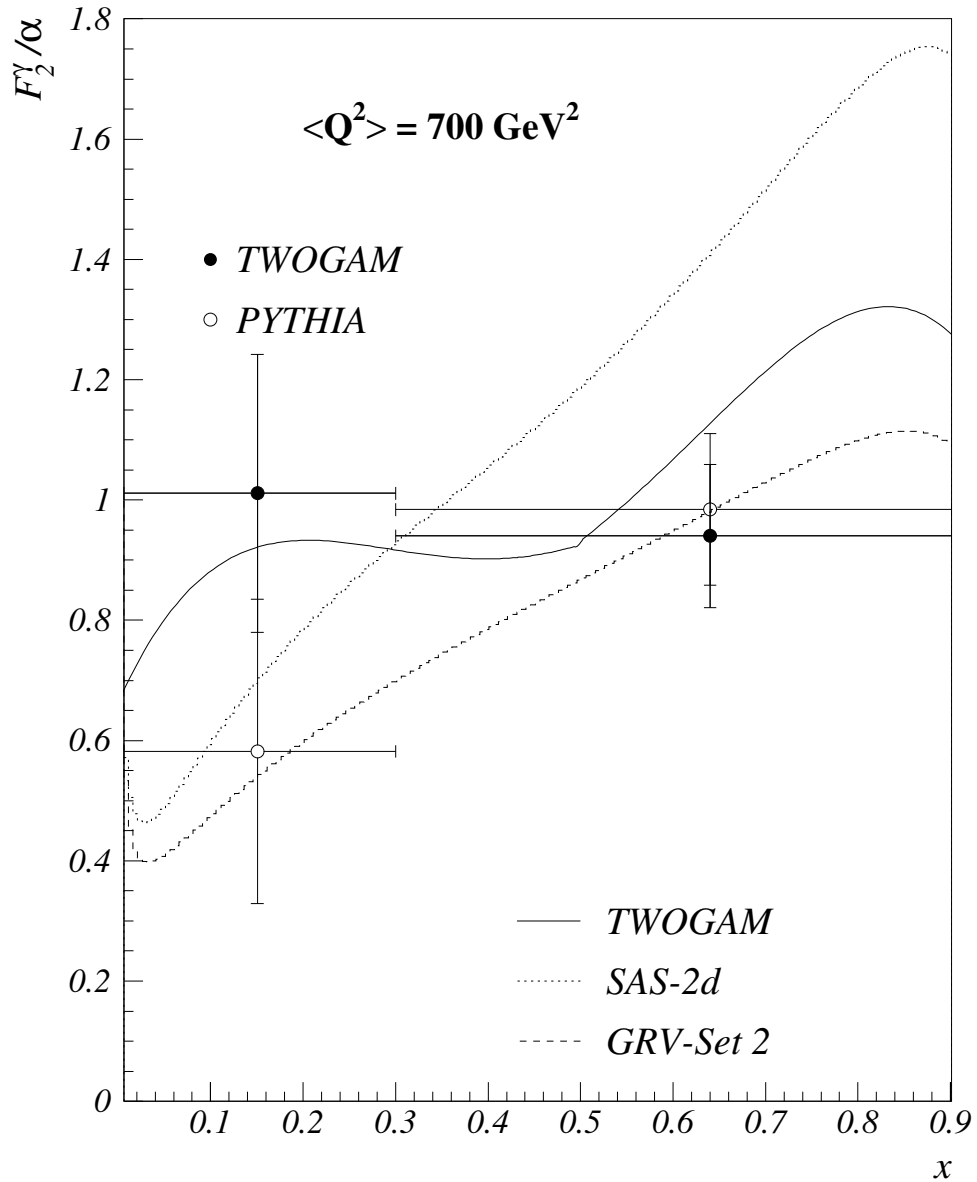


Figure 4: The measured F_2^γ at $Q^2 = 700 \text{ GeV}^2$ as a function of x . Error bars show total errors. The data are compared with the predictions of TWOGAM generator, GRV and SaS models.

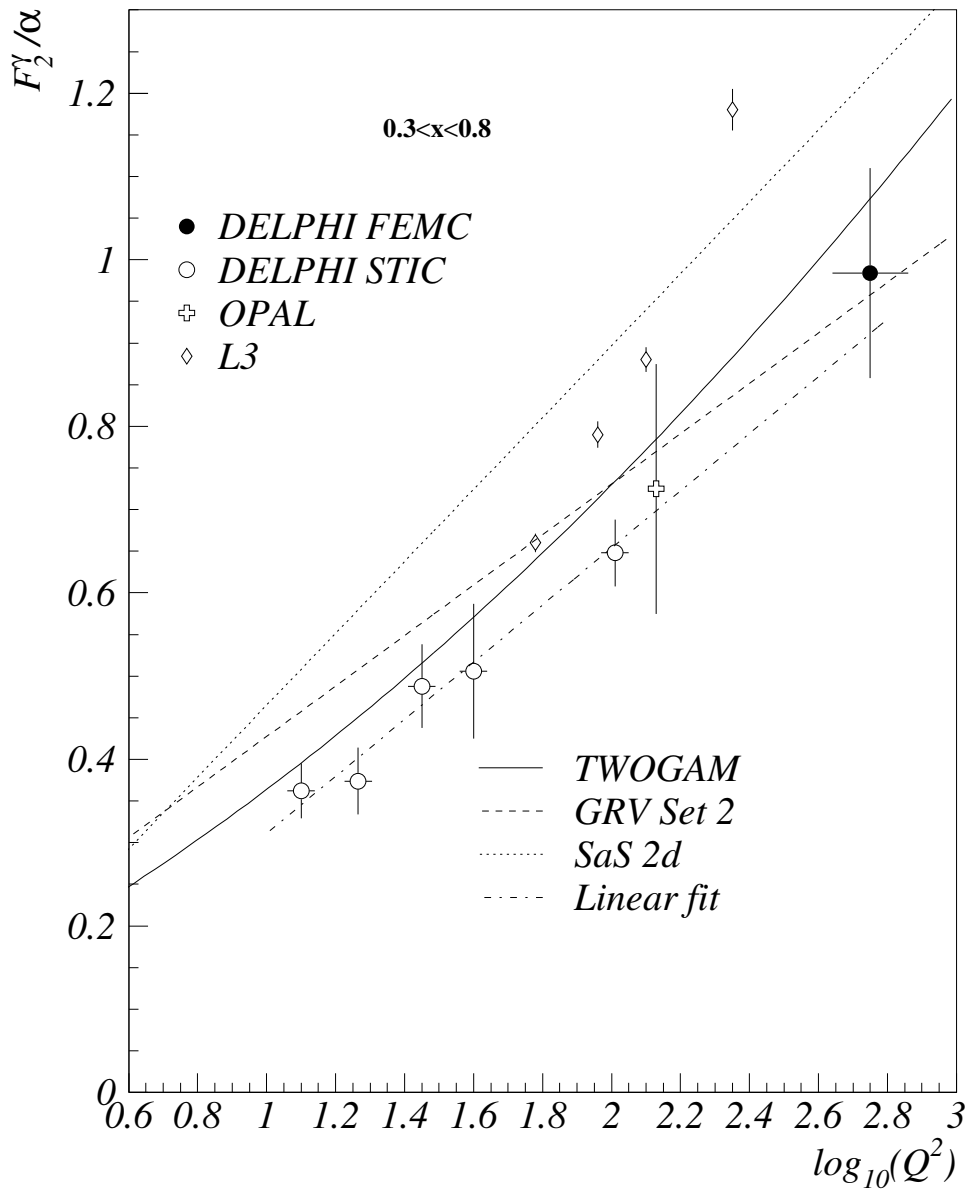


Figure 5: The measured F_2^γ in the x interval 0.3-0.8 as a function of Q^2 compared with predictions of TWOGAM generator, GRV and SaS models and the data from other LEP collaborations. The statistical and systematic errors are added in quadrature.